

Manipulation of multidimensional plasmonic spectra for information storage

Cite as: Appl. Phys. Lett. **98**, 171106 (2011); <https://doi.org/10.1063/1.3584020>

Submitted: 04 February 2011 . Accepted: 04 April 2011 . Published Online: 27 April 2011

Wei Ting Chen, Pin Chieh Wu, Chen Jung Chen, Chun-Jen Weng, Hsin-Chen Lee, Ta-Jen Yen, Chieh-Hsiung Kuan, Masud Mansuripur, and Din Ping Tsai



View Online



Export Citation

ARTICLES YOU MAY BE INTERESTED IN

Invited Article: Broadband highly efficient dielectric metadevices for polarization control
APL Photonics **1**, 030801 (2016); <https://doi.org/10.1063/1.4949007>

All-dielectric phase-change reconfigurable metasurface
Applied Physics Letters **109**, 051103 (2016); <https://doi.org/10.1063/1.4959272>

Electrically tunable all-dielectric optical metasurfaces based on liquid crystals
Applied Physics Letters **110**, 071109 (2017); <https://doi.org/10.1063/1.4976504>



Measure Ready
M91 FastHall™ Controller

A revolutionary new instrument
for complete Hall analysis

Lake Shore
CRYOTRONICS

Manipulation of multidimensional plasmonic spectra for information storage

Wei Ting Chen,¹ Pin Chieh Wu,¹ Chen Jung Chen,¹ Chun-Jen Weng,² Hsin-Chen Lee,³ Ta-Jen Yen,³ Chieh-Hsiung Kuan,⁴ Masud Mansuripur,⁵ and Din Ping Tsai^{1,2,6,a)}

¹Department of Physics, National Taiwan University, Taipei 10617, Taiwan

²Instrument Technology Research Center, National Applied Research Laboratory, Hsinchu 300, Taiwan

³Department of Materials Science and Engineering, National Tsing Hua University, Hsinchu 30013, Taiwan

⁴Department of Electrical Engineering, National Taiwan University, Taipei 10617, Taiwan

⁵College of Optical Sciences, The University of Arizona, Tucson, Arizona 85721, USA

⁶Research Center for Applied Sciences, Academia Sinica, Taipei 11529, Taiwan

(Received 4 February 2011; accepted 4 April 2011; published online 27 April 2011)

We demonstrate a concept of optical data storage through plasmonic resonances of metallic nanostructures. Metallic nanostructures exhibit strong variations in their reflectance and/or transmittance spectra due to surface plasmon polariton resonances. We study the variations in spectra through 50×50 arrays of repeated unit cells covering a total area of $\sim 50 \times 50 \mu\text{m}^2$. Each cell contains ten different nanostructures, such as an ellipse, a ring, a circle, a triangle, a square, etc. The size of each unit-cell is $500 \times 500 \text{ nm}^2$, and the periodicity is $1.0 \mu\text{m}$. The variations in spectra are obvious enough to be distinguished and then retrieved. © 2011 American Institute of Physics. [doi:10.1063/1.3584020]

Optical disk data storage in rewritable phase-change materials in formats such as compact disk, digital versatile disk, and blue ray disk are well-employed in the world.¹⁻⁶ However, due to the diffraction limit, some other methods such as holographic optical storage,⁷ near field optical storage,⁸⁻¹² and three-dimensional optical storage by two-photon excitation¹³⁻¹⁵ have been considered for high-density applications. In recent years, a concept of data storage through plasmonic resonances of metallic nanostructures has also been proposed.^{16,17} Metallic nanostructures exhibit strong variations in their reflectance and/or transmittance spectra due to surface plasmon polariton (SPP) excitation.^{18,19} The SPP resonant modes of a given nanostructure, determined by its material parameters as well as its geometry and dimensions, often exhibit unique features in the optical reflectance/transmittance spectra. The resonances of metallic nanostructures also depend on the polarization state of the incident light, as well as interactions with their environment and with each other. The spectral signature of metallic nanostructures can be used to increase the capacity of optical storage media.^{20,21}

In this letter, we report the results of experiments involving ten different nanostructural features incorporated within a $500 \times 500 \text{ nm}^2$ area. The presence or absence of each such nanostructure gives rise to $2^{10} = 1024$ different reflectance/transmittance spectra when a short pulse (on the order of a few femtoseconds) from a spatially-coherent light source (e.g., super continuum) is focused onto that $500 \times 500 \text{ nm}^2$ area. Assuming one could distinguish 2^{10} different spectra of a given spot during the available time, it should be possible to store and then retrieve ten binary digits (bits) from the area illuminated by a diffraction-limited focused beam. This letter presents the results of a study aimed at proving the feasibility of the concept.

Using electron beam lithography, we fabricated (on a 30-nm-thick gold film on a fused silica substrate) 50×50 arrays of repeated unit cells covering a total area of $\sim 50 \times 50 \mu\text{m}^2$. Each cell contains ten different nanostructures, such as an ellipse, a ring, a circle, a triangle, a square, etc. The size of each unit-cell is $500 \times 500 \text{ nm}^2$, and the periodicity is $1.0 \mu\text{m}$. Figure 1(a) shows the schematic diagram of Espacer (Kokusai Eisei Co., Showa Denso Group, Japan)/poly methyl methacrylate (PMMA-495K) bilayered resist fabrication process. The detail of fabrication process is simi-

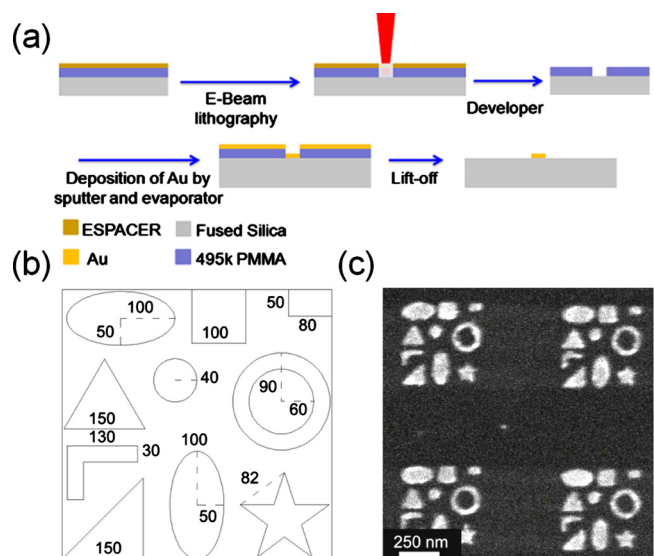


FIG. 1. (Color online) (a) Schematic diagram showing the process of e-beam lithography. Our samples were fabricated without any adhesion layer (such as Ti or Cr) between the gold film and the glass substrate. A 3 nm film of gold was sputter-deposited on the developed resist layer, followed by thermal evaporation of another 27 nm layer of gold. (b) Diagram showing the dimensions (in nm) of each nanostructure embedded within a single $500 \times 500 \text{ nm}^2$ unit-cell. (c) SEM image of a small region from the fabricated sample. This array contains four repetitions of ten different nanopatterns with a periodicity of $1.0 \mu\text{m}$ along both horizontal and vertical axes.

^{a)}Electronic mail: dptsai@phys.ntu.edu.tw.

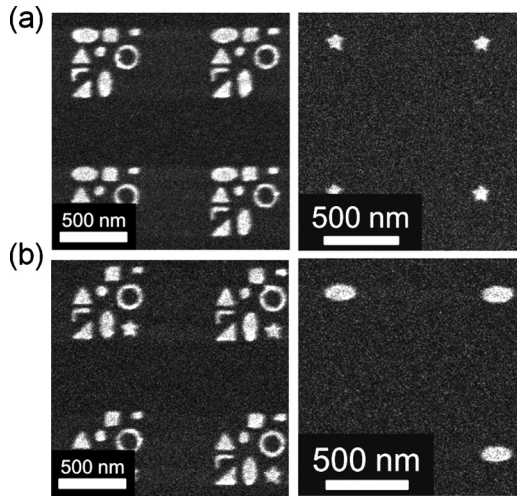


FIG. 2. SEM images of small regions from four different fabricated samples in which each unit cell is missing a star (upper left), or an ellipse (lower left), or the unit cell contains only a single star (upper right), or a single ellipse (lower right).

lar to our prior work.²² Figure 1(c) shows a scanning electron microscope (SEM) image of a small region of a sample containing four unit cells; dimensions (in nanometer) of the various features within each cell are specified in the diagram of Fig. 1(b).

We also fabricated some arrays by removing one and only one nanofeature from each and every unit cell in order to examine the differences of the spectra. For example, removing the nanostar from the lower right-hand-side of each cell in Fig. 1(c) yields the periodic pattern depicted in the upper-left-hand frame of Fig. 2. We also examined the spectra of periodic arrays of unit-cells that contain only one of the ten nanofeatures, such as that seen in the SEM image in the lower-right-hand frame of Fig. 2, which shows each of

the four unit-cells containing a single nanoellipse and nothing else.

Transmittance spectra in the wavelength range $\lambda = 400$ nm to 1050 nm using x- and y-polarized illumination were measured using a B&W Tek Inc. BRC642E spectrometer combined with Carl Zeiss Axio microscope (10 \times objective, numerical aperture NA=0.3, 100 W halogen light source). The transmittance spectra are normalized by the transmissivity of an unpatterned region of the fused silica wafer. Figures 3(a) and 3(b) show the transmittance spectra of the arrays illuminated at normal incidence using x- and y-polarized light, respectively. In these figures, the spectrum depicted in black corresponds to the sample with all ten nanofeatures present [i.e., the sample shown in Fig. 1(c)], whereas those depicted in color represent samples in which one of the nanofeatures (namely, star, ring, ellipse, triangle, etc.) has been removed; for typical SEM images of such samples see the left-hand column of Fig. 2. In Figs. 3(c) and 3(d), the color spectra correspond to samples which contain, within each repeated unit cell, a single feature, e.g., a star, a ring, an ellipse, or a triangle; for typical SEM images of such samples see the right-hand column of Fig. 2.

As might have been expected, the various spectra differ from one another for x- and y-polarized illumination. For example, in the case of x-polarized illumination in Fig. 3(a), comparing the spectrum in pink with that in black, a little peak appeared at $\lambda \sim 600$ nm, and the dip at $\lambda \sim 880$ nm became sharper. These two variations in spectra resulted from removing the surface plasmon resonances of the nanoellipse. The pink spectrum in Fig. 3(c) shows the plasmon resonance of the nanoellipse with major axis along the perpendicular direction: there are two plasmon resonances at $\lambda \sim 613$ nm and $\lambda \sim 950$ nm under x-polarized illumination. Therefore, the intensity of the black curve in Fig. 3(a) at $\lambda \sim 613$ nm and $\lambda \sim 950$ nm should be enhanced when this nanoellipse is removed. Similarly, removing the nanotriangle

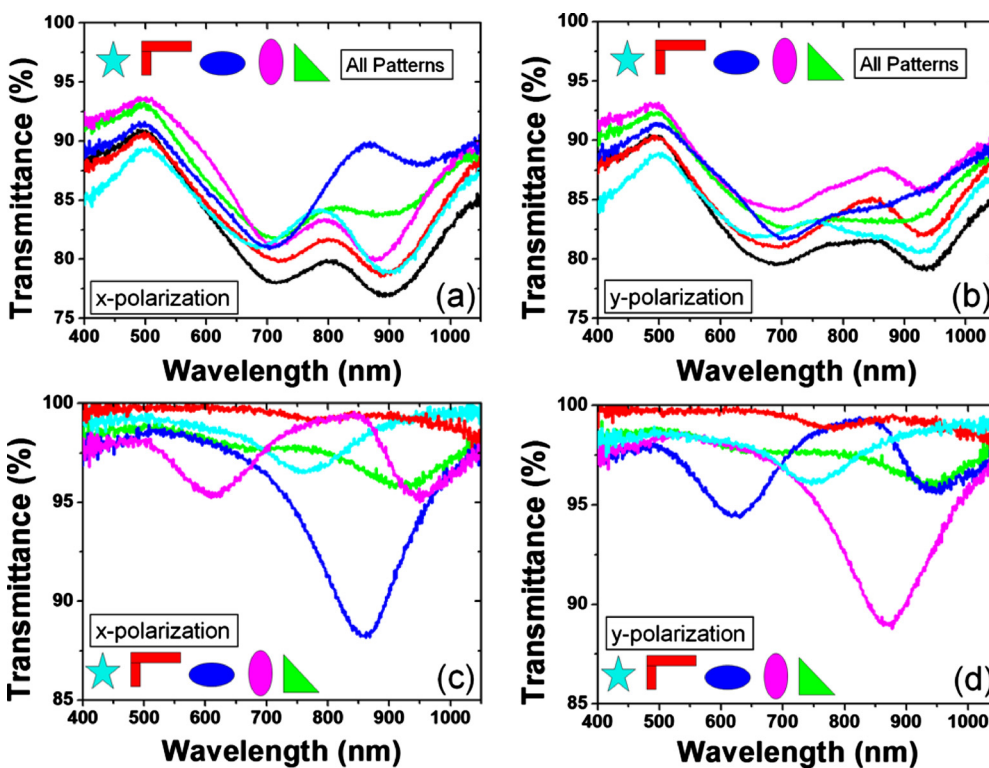


FIG. 3. (Color online) Transmittance spectra of periodic arrays of identical unit-cells for x- and y-polarized illumination, each containing different nanofeatures. In frames [(a) and (b)], the black spectrum corresponds to complete unit cells having all ten nanofeatures, whereas colored spectra represent unit-cells with one feature removed; the missing feature is indicated in the legend. Frames (c) and (d) represent unit-cells containing a single nanofeature; the color (matched to the legend) identifies the nanofeature.

or the nanoellipse having its major axis along the horizontal direction, weakens the intensity of the black spectrum at $\lambda \sim 889$ nm.

In Fig. 3(a), aside from the overall change in transmitted intensity, no obvious changes are observed when removing the L-shaped nanofeature (red) or the nanostar (light blue) with x-polarized illumination. However, in Fig. 3(b), corresponding to y-polarized illumination, comparing the spectrum in black with the spectrum in light blue, a peak at $\lambda \sim 744$ nm appears when the nanostar is removed. Similarly, by removing the L-shaped nanostructure, the peak at $\lambda \sim 845$ nm becomes more distinct than that of the black spectrum. These variations in the light-blue and the red spectra originate, respectively, from the plasmonic resonances of the nanostar and the L-shaped nanofeature. The peak in the light-blue spectrum at $\lambda \sim 744$ nm in Fig. 3(b), for example, originate from removing the plasmonic resonance of the nanostar seen in the light-blue curve of Fig. 3(d).

We emphasize that our explanations of the observed spectral changes arising from the removal of specific nanofeatures are only qualitative. One would need to conduct a suitable set of control experiments along with detailed numerical analyses in order to better understand the physics that underlies these observations. On general grounds, one expects that the removal of a nanofeature would be seen most dramatically at and near those wavelengths at which the (isolated) nanofeature exhibits plasmonic resonances. However, it is also true that each nanofeature interacts with its neighborhood so much, so that the resulting spectrum is a complex function of the shapes and dimensions of the neighboring nanofeatures—not to mention the polarization state of the incident light. To the extent that such interactions occur in practice (via the excitation of short-range as well as longer-range surface plasmon polaritons within neighboring structures), the spectral changes observed in consequence of the removal of a single feature would depend not only on the feature itself, but also on its position among the surrounding nanofeatures.

Similar spectral variations are observed upon removing the nanoellipses when illumination has a given state of polarization. Intriguingly, we find that the variations in spectra while removing the ellipse having its major axis along the x-axis under x-polarized illumination [see the blue spectrum in Fig. 3(a)] are different from those obtained when removing the ellipse having its major axis along the y-axis under y-polarized illumination [see the pink spectrum in Fig. 3(b)]. This obvious spectral variation results from the coupling of the nanoellipse with nanoparticles in its vicinity rather than from any fabrication variations in the nanoellipses. In Fig. 1(c), the shapes of the ellipses with major axes along the x- and y-directions are slightly different; however, this structural variation does not appear to change the corresponding plasmonic resonances substantively, as may be confirmed by comparing the blue and pink spectra of Fig. 3(c) with those of Fig. 3(d). The ellipse having its major axis along the x-direction is very close to the square on its right and the triangle on its lower side so that the coupling effect of the ellipse with the square and the triangle is particularly strong. The change in the spectrum is clearly visible when the nanoellipse with its long axis along the x-direction is removed. This feature of plasmonic resonance provides the possibility of enhancing the spectral variations for optical data storage

through the coupling effect of nanoparticles, a feature that is especially suited for high-density data storage applications. In the case of conventional optical storage, the signal obtained from recorded marks becomes less distinct when marks come closer together within a diffraction-limited spot. In the case of information storage through plasmonic resonances, however, readout signals become easier to detect when two nearby metallic nanostructures interact.

We studied the concept of high-density optical data storage by employing plasmonic resonances. The SPP-induced changes in spectra corresponding to different shapes and orientations of metallic nanoparticles illuminated by x- and y-polarized light can be employed to enhance the capacity of information storage media. The transmittance spectra were seen to change their intensity as well as their profiles when different combinations of nanoparticles were present in a unit-cell. Unlike the restrictions imposed on conventional optical storage by the diffraction limit of light, the spectral variations become enhanced when nanoparticles within a unit-cell come closer together. This characteristic seems to be especially suitable for high-density optical storage when exploiting plasmonic resonances.

The authors thank financial aids from NSC, Taiwan, under Grant Nos. 99-2811-M-002-003, 99-2120-M-002-012, 99-2911-I-002-127, and 98-EC-17-A-09-S1-019. Technical help from Mr. Shian-Wen Chang of Instrument Technology Research Center and Mr. Fu-Min Wang of National Taiwan University are especially appreciated.

- ¹C. H. Chu, C. D. Chiun, H. W. Cheng, M. L. Tseng, H. P. Chiang, M. Mansuripur, and D. P. Tsai, *Opt. Express* **18**, 18383 (2010).
- ²H. J. Borg, M. van Schijndel, J. C. N. Rijpers, M. H. R. Lankhorst, G. F. Zhou, M. J. Dekker, I. P. D. Ubbens, and M. Kuijper, *Jpn. J. Appl. Phys., Part 1* **40**, 1592 (2001).
- ³T. Ohta, *J. Optoelectron. Adv. Mater.* **3**, 609 (2001).
- ⁴S. K. Lin, I. C. Lin, S. Y. Chen, H. W. Hsu, and D. P. Tsai, *IEEE Trans. Magn.* **43**, 861 (2007).
- ⁵L. P. Shi, T. C. Chong, P. K. Tan, X. S. Miao, J. J. Ho, and Y. J. Wu, *Jpn. J. Appl. Phys., Part 1* **39**, 733 (2000).
- ⁶I. Satoh, S. Ohara, N. Akahira, and M. Takenaga, *IEEE Trans. Magn.* **34**, 337 (1998).
- ⁷J. F. Heanue, M. C. Bashaw, and L. Hesselink, *Science* **265**, 749 (1994).
- ⁸W. C. Lin, T. S. Kao, H. H. Chang, Y. H. Lin, Y. H. Fu, C. T. Wu, K. H. Chen, and D. P. Tsai, *Jpn. J. Appl. Phys., Part 1* **42**, 1029 (2003).
- ⁹D. P. Tsai and W. R. Guo, *J. Vac. Sci. Technol. A* **15**, 1442 (1997).
- ¹⁰J. Tominaga, T. Nakano, and N. Atoda, *Appl. Phys. Lett.* **73**, 2078 (1998).
- ¹¹K. P. Chiu, K. F. Lai, and D. P. Tsai, *Opt. Express* **16**, 13885 (2008).
- ¹²Y. S. Kim, S. J. Lee, Y. J. Kim, N. C. Park, and Y. P. Park, *Jpn. J. Appl. Phys., Part 1* **43**, 5756 (2004).
- ¹³J. H. Strickler and W. W. Webb, *Opt. Lett.* **16**, 1780 (1991).
- ¹⁴S. Kawata and Y. Kawata, *Chem. Rev. (Washington, D.C.)* **100**, 1777 (2000).
- ¹⁵D. Day, M. Gu, and A. Smallridge, *Adv. Mater. (Weinheim, Ger.)* **13**, 1005 (2001).
- ¹⁶P. Zijlstra, J. W. M. Chon, and M. Gu, *Nature (London)* **459**, 410 (2009).
- ¹⁷D. O'Connor and A. V. Zayats, *Nat. Nanotechnol.* **5**, 482 (2010).
- ¹⁸T. W. Ebbesen, H. J. Lezec, H. F. Ghaemi, T. Thio, and P. A. Wolff, *Nature (London)* **391**, 667 (1998).
- ¹⁹A. R. Zakharian, M. Mansuripur, and J. V. Moloney, *Opt. Express* **12**, 2631 (2004).
- ²⁰M. Mansuripur, A. R. Zakharian, A. Lesuffleur, S. H. Oh, R. J. Jones, N. C. Lindquist, H. Im, A. Kobayakov, and J. V. Moloney, *Opt. Express* **17**, 14001 (2009).
- ²¹S. Park and J. W. Hahn, *Opt. Express* **17**, 20203 (2009).
- ²²W. T. Chen, P. C. Wu, C. J. Chen, H. Y. Chung, Y. F. Chau, C. H. Kuan, and D. P. Tsai, *Opt. Express* **18**, 19665 (2010).